11th ANKARA INTERNATIONAL AEROSPACE CONFERENCE
8-10 September 2021 - METU, Ankara TURKEY

**AIAC-2021-122**

# NUMERICAL COMPUTATION OF MAXIMUM AERODYNAMIC LOADS FOR ENGINE INTAKE IN SUPERSONIC AIRCRAFT

Muhammed Osama BALKHI [1],
Sehle CENGIZ[2]
Samsun University
Samsun, Turkey

Ali Han YILDIRIM[3]
TUSAS
Istanbul, Turkey

Ahmet Selim DURNA[4]
University of Samsun
Samsun, Turkey

## ABSTRACT

*In this study, the RAE M2129 engine intake flow analysis will be carried out in steady flows. Hammershocks that can form in the engine at high speeds will also be examined. Hammershocks are a kind of reverse flow interaction in supersonic aircraft that causes a large and transient pressure increase along the duct on the engine compressor face in the direction opposite to the flow rapidly. The research was examine a supersonic aircraft intake which was analyzed with computational methods. The solutions were found to be compatible with the historically experimental and numerical data.*

## INTRODUCTION

As the air is introduced to the engine through the air intake, air intake design is considered one of the most important performance parameters. The primary purpose of air intake is to provide the compressor with a uniform airflow in certain conditions required by the engine while maximizing efficiency. [Ramasamy, Mahendran, Vijayan, 2009] However, in some cases, the angle of attack of the compressor vanes can change the angle of flow, which can cause a stall. [Benser, Finger, 1957] In such a case, the effect of a wall on the surface of the compressor occurs and shock waves called "hammershock" occur in the direction opposite to the flow. This shock wave is one of the critical situations occurring in the input channel and its destructive effect is much larger especially for aircraft flying at high speeds. [Menzies, 2002] This phenomenon should be considered from the outset of preliminary design and necessary analysis should be done to create the appropriate channel to withstand shock-related design loads. Technically, a hammershock is an engine reverse that causes reverse flow between the compressor surface and the inlet which creates a high transient pressure increase at the motor compressor surface. [Nugent, Holzman, 1974] This reverse flow, which occurs after the Hammershock, spreads rapidly towards the inlet. During this propagation, it creates high loads and temperature differences on both the duct and the engine. This temporary pressure increase is called a hammershock. [Menzies, 2002] During the design phase of the propulsion system, the phenomenon of hammershock should be carefully studied and design criteria should be set accordingly to minimize any reverse flow and pressure surge. [Becker, Bergmann, Luber, 1994] The design of an aircraft intake often depends on the conditions under

[1] Undergraduate Researcher, Email: 16960090@samsun.edu.tr
[2] Undergraduate Researcher, Email: 16960054@ samsun.edu.tr
[3] Design Engineer, Email: alihan.yildirim@tai.com.tr
[4] Assist. Prof. in Aerospace Engineering Department, Email: ahmetselim.durna@samsun.edu.tr

which the aircraft will operate but may also depend on the specific role of the aircraft, the layout of the storage locations, and the location of the landing gear wells. [Laruelle, 2002] In previous years, data on engine air intake design has mostly been derived from wind tunnel tests. Any problems that occurred, such as damage to the entrance structures as a result of engine surges, tended to be detected only after prototype testing and flight. Computational techniques were also widely used, and CFD simulations of aircraft inflows contributed to the understanding of inflow physics with the development of wind tunnel testing methods. [Hinton, Eastlake, 1998] CFD methods have advantages over experimental techniques as they are generally cheaper in terms of cost, time, and resources. However, some problems are difficult to study experimentally, often at large expense and requiring a full-scale facility to do so, and in such cases, CFD can be considered as a viable alternative. CFD can also aid in understanding experimental problems that allow results to be verified. [Versteeg, Malalasekera, 1995]

In order to foresee these conditions, experiments and computational studies regarding the case are demanded, and air intakes with maximum efficiency are required to prevent the formation of a hammershock or minimize its effects. In this study, an S-Shaped inlet (S-Shaped ducts) is examined and a CFD study is performed. RAE Model 2129 S-shaped inlet geometry is used as a reference for the CFD analysis. Hammershock effects on this inlet and its parameters will be examined. Results will be compared with historical experimental and computational data.

## METHOD

### Geometry

Figure 1 shows the required parameters to define the geometry of the RAE M2129 model. In order to construct the geometry, the curve equation of Equation 2 was used. [Anderson, Reddy, Kapoor, 1993] The drawing is extruded since the values of the input and output fields are determined. Then NACA 1-854-35 airfoil was used, except at the upstream section of the intake. The three-dimensional configuration of the geometry was shown in Figure 2.

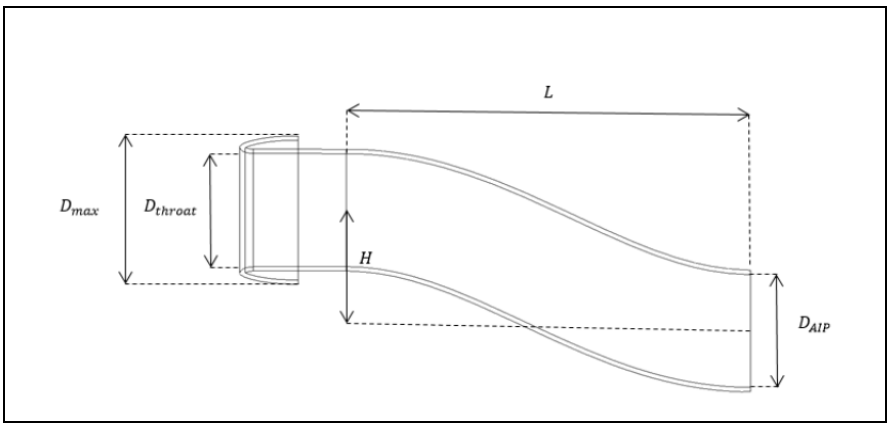


**Figure 1*:*** RAE M2129 intake geometry

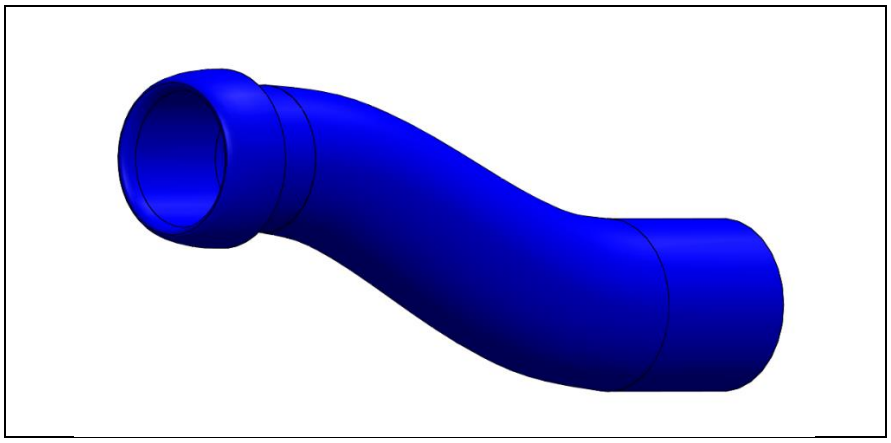

**Figure 2***:* RAE M2129 3D geometry

$$y = 0.0 \tag{1}$$

$$z = -0.15\left(1.0 - \cos\left(\frac{\pi x}{L}\right)\right) \tag{2}$$

where x takes values between 0 and L, where L is the duct length. The throat diameter and the engine phase diameter are denoted by $D_{throat}$ and $D_{AIP}$ respectively. The location of the aerodynamic interface plane is referred to as $X_{AIP}$. Required measurements are provided in Table 1. [Anderson, Reddy, Kapoor, 1993]

**Table 1:** Dimensions of M2129 intake geometry [Anderson, Reddy, Kapoor, 1993]

| Parameters | Value (mm) | Description |
|---|---|---|
| $D_{throat}$ | 128.80 | Throat diameter |
| $D_{max}$ | 168.68 | Maximum diameter |
| $D_{AIM}$ | 152.40 | Diameter at the engine face |
| *L* | 457.20 | Duct length |
| *H* | 137.16 | Distance between centers |

**Grid Generation**

In order to generate a structure grid to the S-duct geometry of RAE M2129, first, the model was drawn using Solidworks with the domain as shown in Figure 3. Subsequently, the model was imported to ICEM CFD to generate the grid. A structure grid with O topology was created. A total of 37 blocks were generated and ICEM CFD HEXA was used to compose the grid. A value of unity or less was set for the y+ parameter and the first layer thickness was calculated accordingly. A total of 8458232 elements were created. The maximum aspect ratio was found as 903, which is normal due to the usage of small elements near the wall to model the boundary layer.

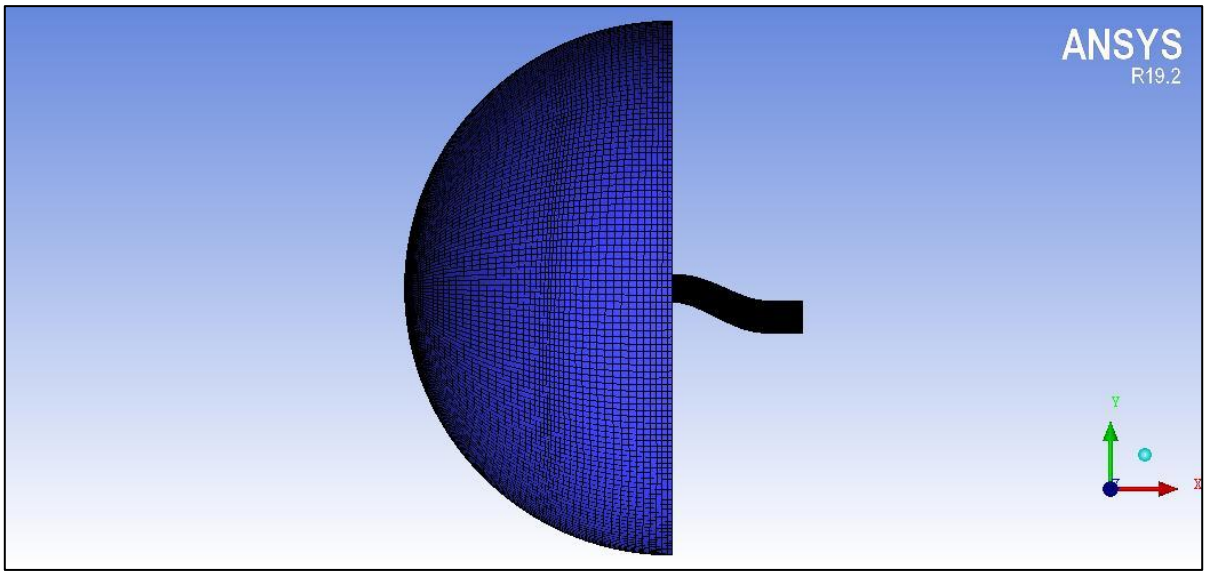


**a)**

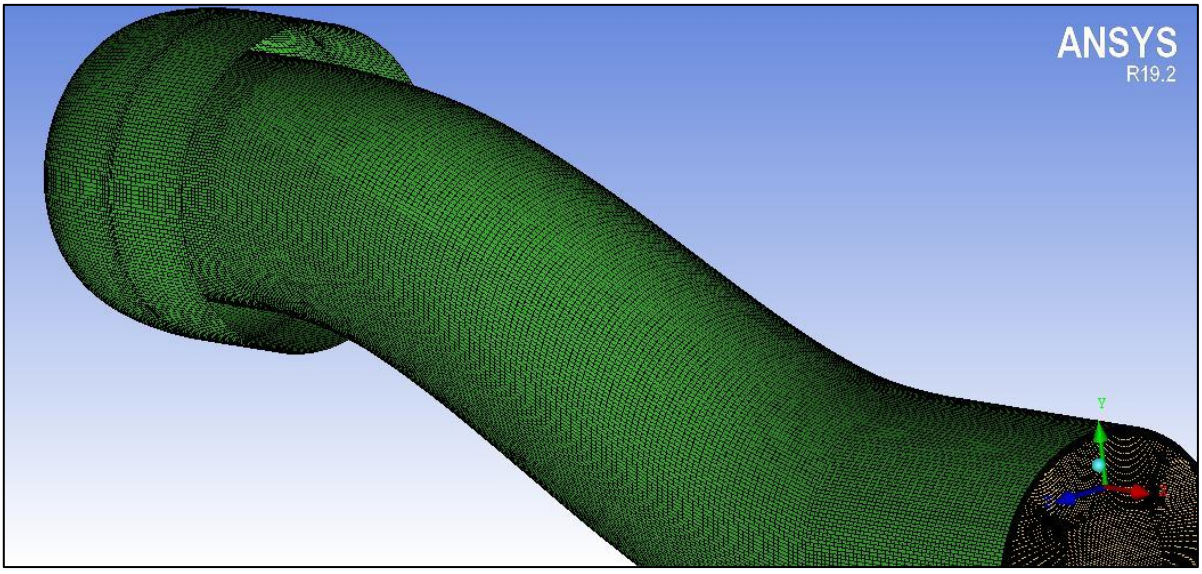


**b)**

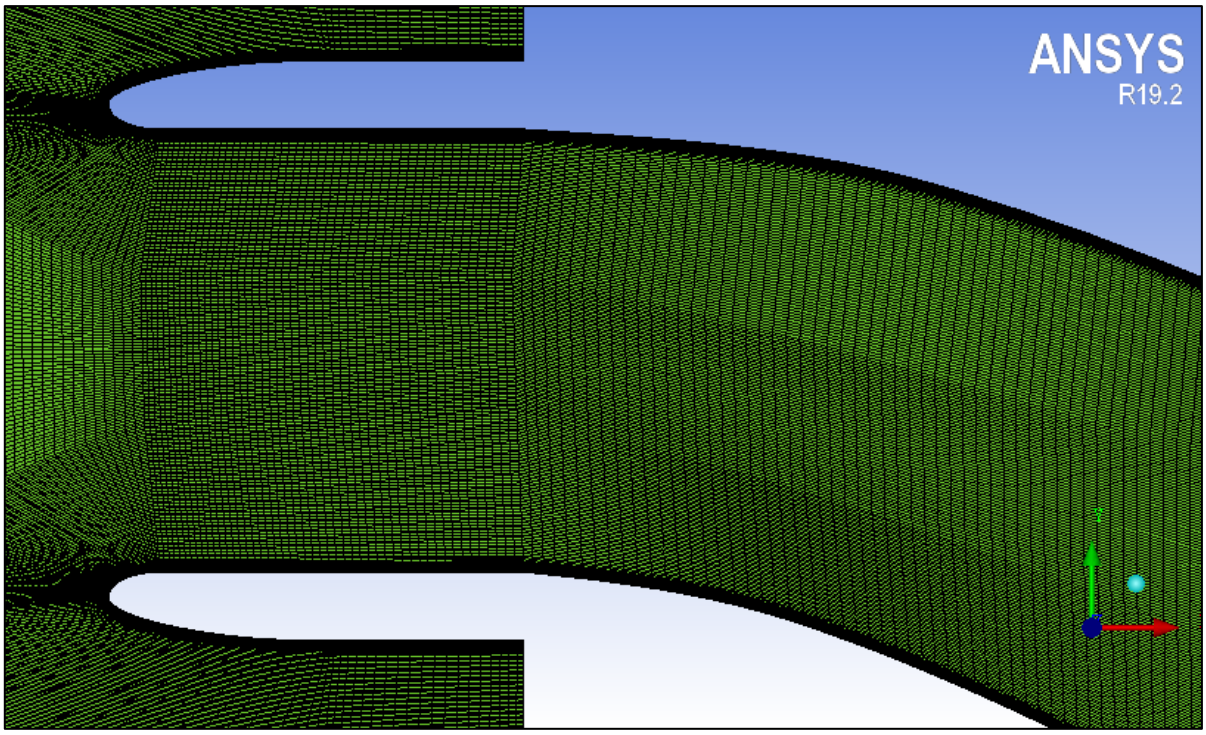


**c)**

**Figure 3:** a) Domain of the grid b) Face mesh on S-duct c) Grid density for z-axis cross-section

**Numerical Methods**

To analyze the motion of a fluid element, the governing equations of fluid dynamics, Navier-Stokes equations were used. The Navier-Stokes equations form a system of non-linear partial differential equations in their full form, which is not analytically solvable. It is however possible to obtain approximate solutions through computational methods, giving rise to Computational Fluid Dynamics, or CFD. The k-w model has been widely used and successful results were obtained for 2-dimensional flows with adverse and favorable pressure gradients. The aforementioned model is going to be used in this work. It has also been found that the model tends to be consistent with the calculated properties of the recirculating flow without altering the basic model and its coefficients of closure. When used in flows with boundary layer separation caused by an interaction with a shock wave, problems found with the model involve unreliability. [Wilcox, 1689-1699] In the solution part of the analysis, a density-based solver was selected and k-w (SST) was used for viscous settings. The boundary conditions were calculated using the isentropic relations and were shown in Table 2.

**Table 2:** Boundary Condition

| Parameters | Value | Description |
|---|---|---|
| Mach Number | 0.21 | Inlet (Pressure Far-Field) |
| Gauge Pressure | 98152.286 Pa | Inlet (Pressure Far-Field) |
| Temperature | 290.438 K | Inlet (Pressure Far-Field) |
| Total Gauge Pressure | 93928.28 Pa | Outlet (Pressure Outlet) |
| Temperature | 293 K | Outlet (Pressure Outlet) |

The pressure farfield, pressure outlet and wall boundary conditions were defined for the flow domain inlet, engine face and the intake geometry, respectively. Second-order upwind was selected for the solution method.

## RESULTS AND DISCUSSION

In order to validate the results of this study, a test case of AGARD of a steady flow problem was considered and the results were compared with previous experimental and computational studies. This case is shown in Table 3.1

**Table 3: AGARD Test Case 3.1**

| Test Case | Mach Number | Pressure Recovery | Mass Flow Rate (MFR) | Contraction Ratio |
|---|---|---|---|---|
| 3.1 | 0.21 | 0.9280 | 2.173 | 0.9312 |

55000 core-hours and 98 GB of disk data storage space were purchased from the National High-Performance Computing Center (UHEM), which serves both academic and industrial users, to perform the analysis provided by this study.

For comparison purposes, the upper and lower curves of S-shaped air intake geometry were defined as the port and starboard sides, respectively. This was demonstrated in figure 5. The Mach number contour was given in Figure 6.a and it was observed that the flow accelerates immediately after the stopping point, on the leading edge of both the port and the starboard part.

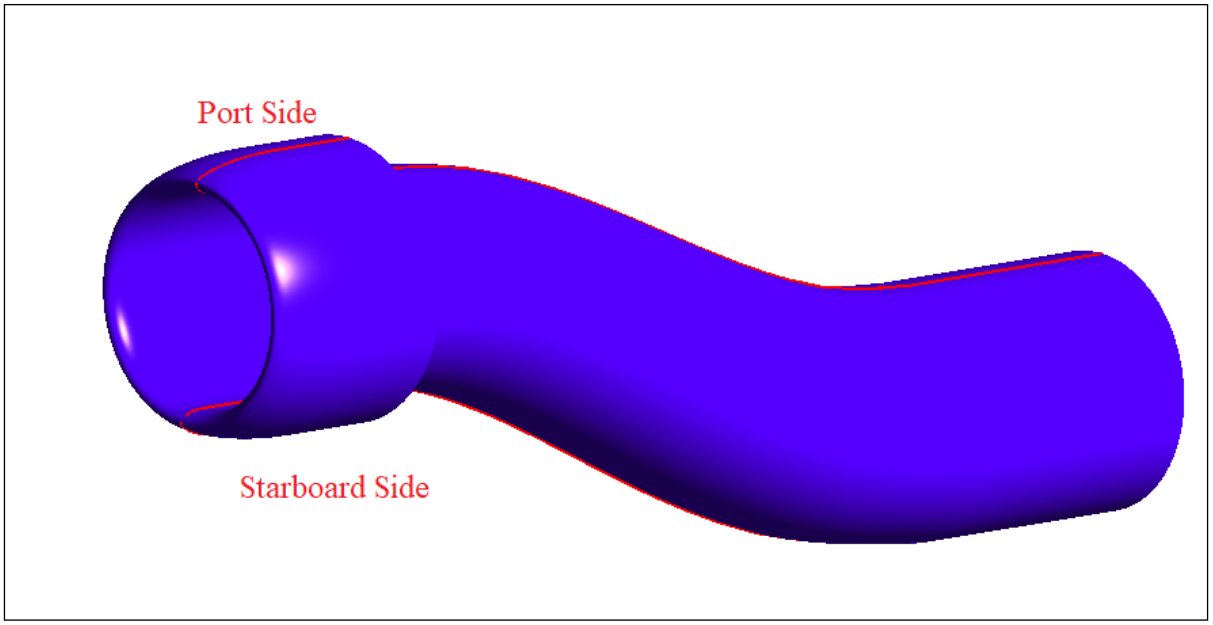


**Figure 5:** Demonstration of Port and Starboard sides

It was observed that results given in [Menzies, 2002] are quite compatible with the Mach number contour obtained in Figure 6. The positions, sizes and shapes of the shock waves and their interactions are matching. After the point where the S-shaped slope of the air intake begins, flow separation occurs. It was observed that this current separation takes a larger area up to the motor input and a similar current separation width occurs both in our study and in [Menzies, 2002] numerical solutions.

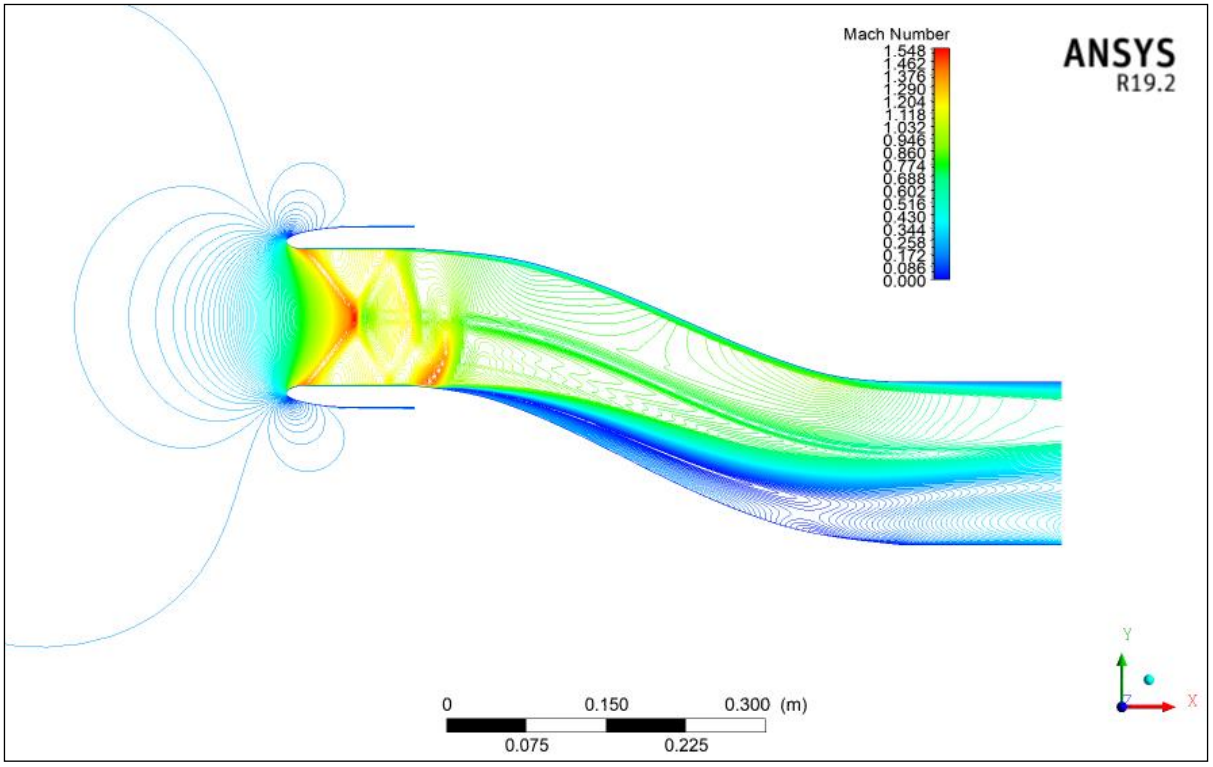


**a)**

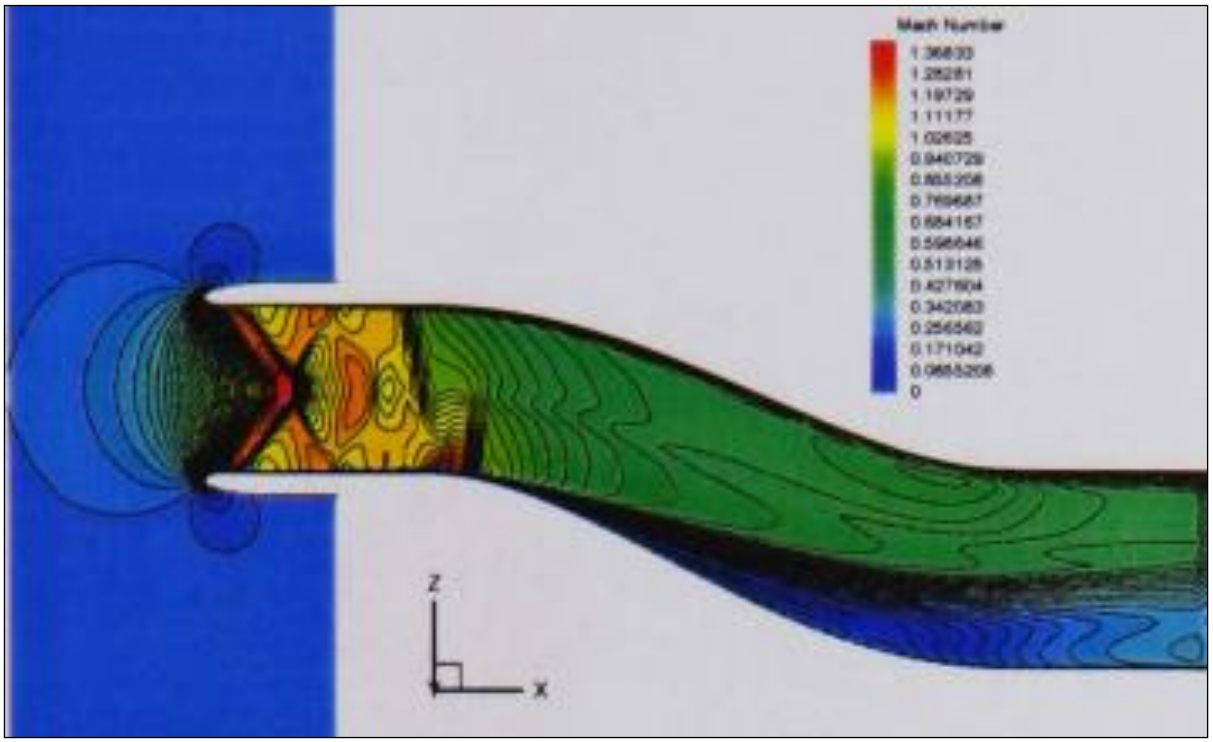


**b)**

**Figure 6:** Mach contour a) This study (HMFR) b) Menzies [Menzies, 2002]

In Figure 7.a, the total pressure recovery contour was given in the circular section taken from the engine face in the direction perpendicular to the flow. A circular region with low-pressure recovery, shown in blue, was formed in the acquired contour. It was observed that the result is quite compatible with Menzies' study shown in Figure 7.b. The circular area of the flow

separation was noted to be larger in this study, resulting in the formation of a large circular area where the pressure gain had its lowest values.

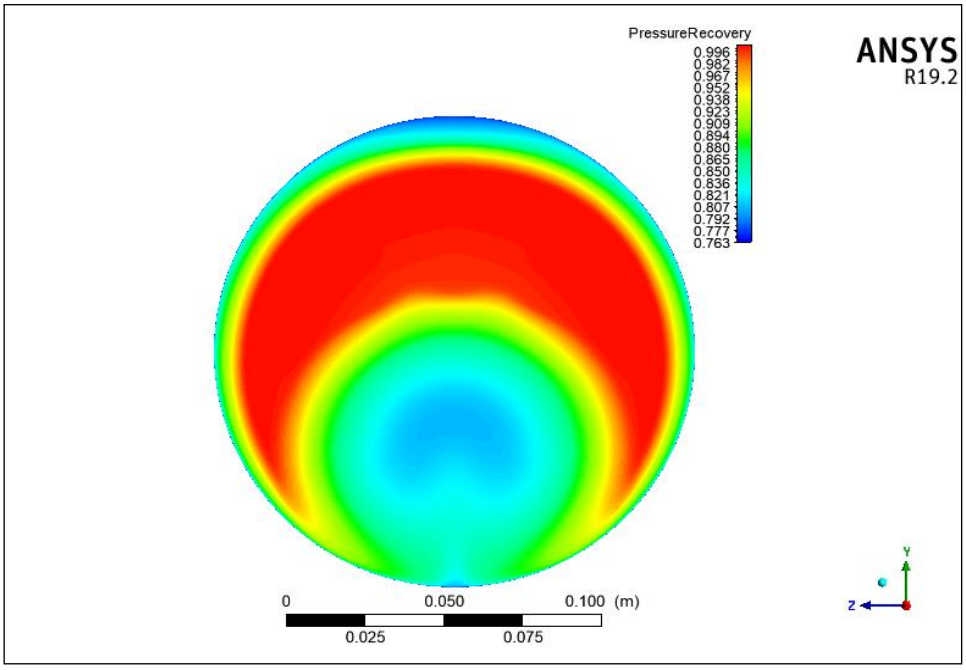


**a)**

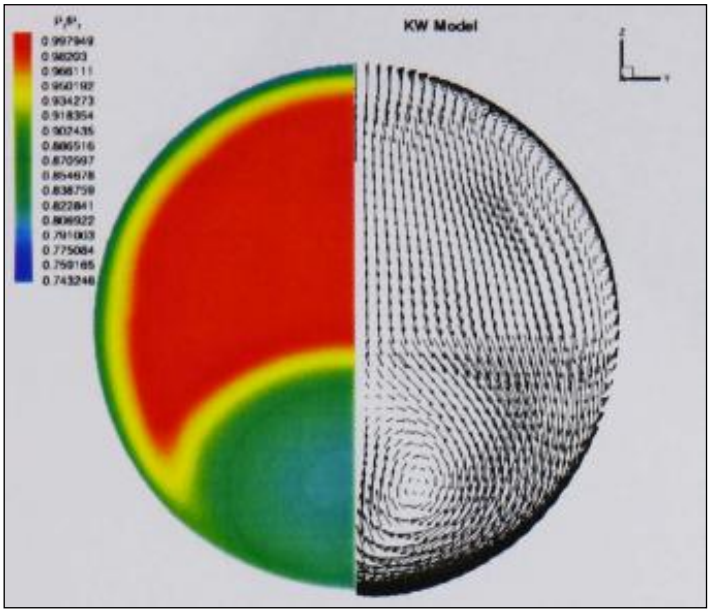


**b)**

**Figure 7:** Pressure recovery in the section taken at the engine face a) This study (HMFR) b) Menzies [Menzies, 2002]

Finally, the pressure distribution taken along the port and starboard sides was given comparatively, together with the results of the previous experimental and numerical results. These experimental and numerical solutions were referenced from the Defense Evaluation and Research Agency (DERA) and AGARD Test Report. [DERA, 2001] [Breuer, Servaty, 1996] The experiments were referred to as "ARA Experiment" and "BAe Experiment", respectively. The results obtained were compared to the previously mentioned experiments, and the numerical solutions of Menzies and ARA.

The x-axis represents the dimensionless length X/D while the y-axis represents the dimensionless pressure Ps/PT (Ps=Static pressure, PT=Total pressure at the inlet) for both the port and starboard sides. The pressure distribution along the duct for the port side in Figure 9 and the starboard side in Figure 10 were shown comparatively. In both figures, experimental data and numerical studies were illustrated as points and curves respectively. The numerical solution (red curve) represents the solutions proposed in this study which appears to be in good agreement with the experimental results of Bae, and the curve trend showed consistency with all the results of the other studies.

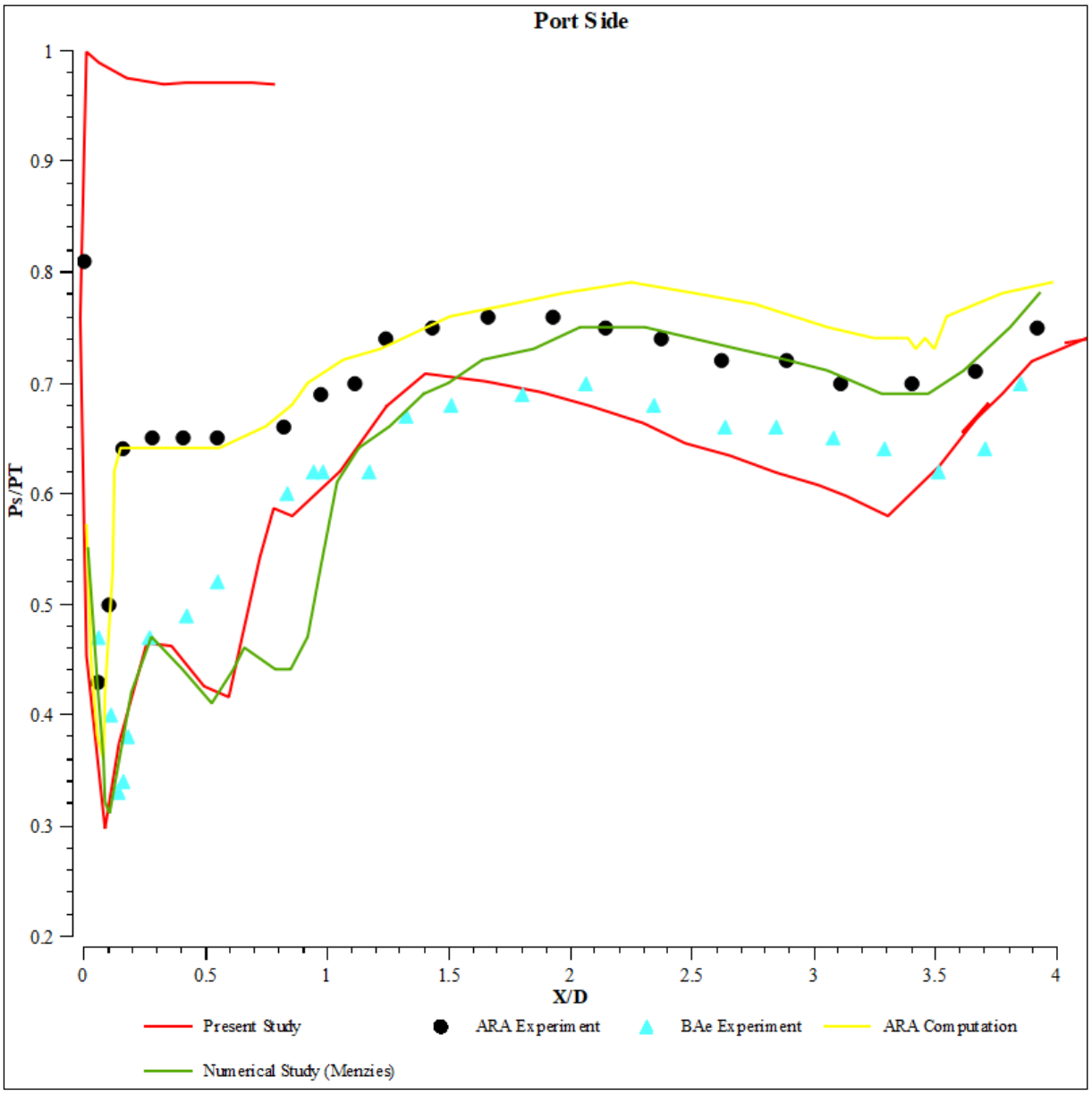


**Figure 9:** Comparison of pressure distribution along the channel for the port section (HMFR)

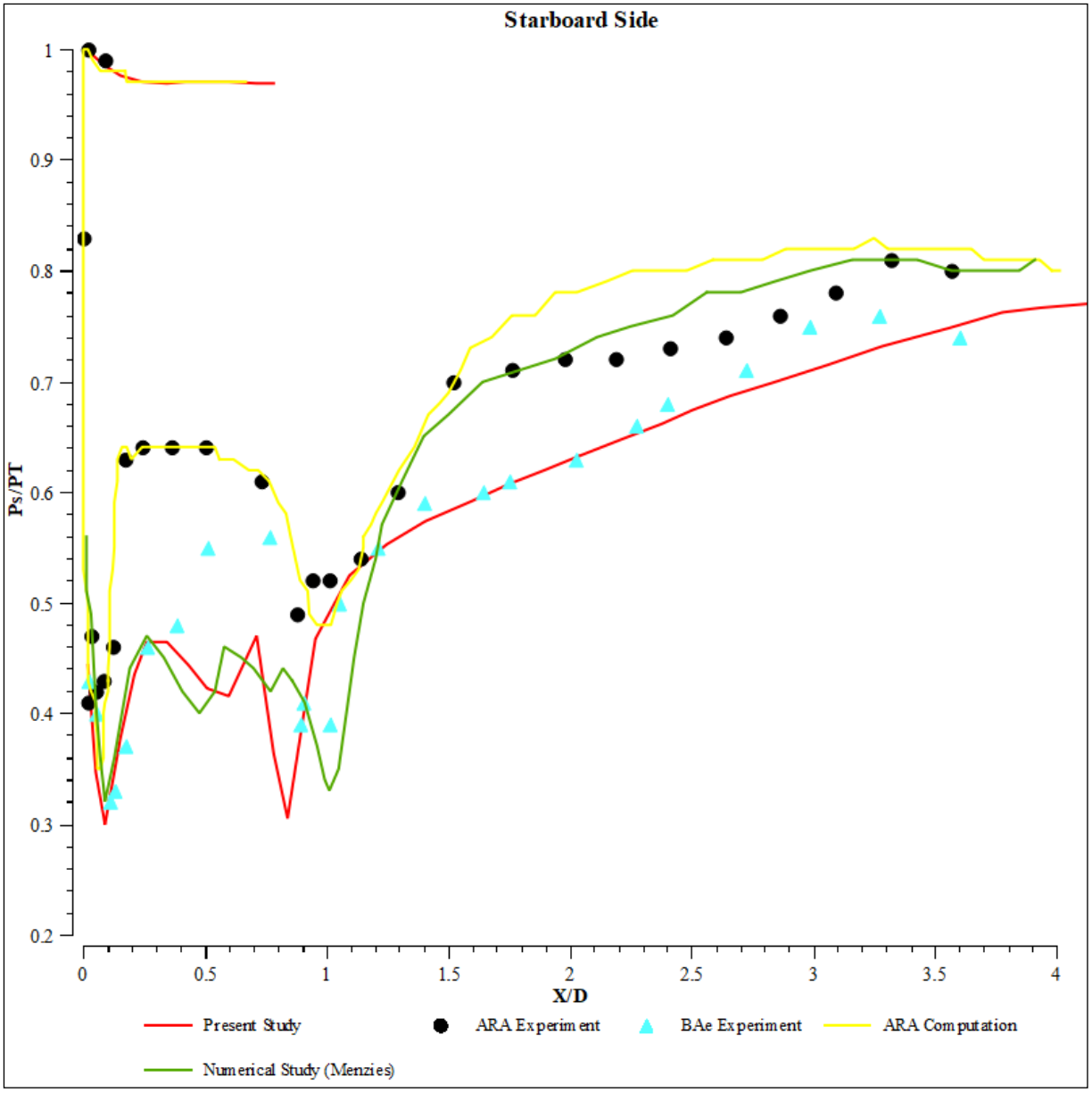


**Figure 10:** Comparison of pressure distribution along the channel for the starboard section (HMFR)

## CONCLUSION AND FUTURE WORKS

To validate the results of this study, the test case of the high mass flow rate has been examined. The k- w SST turbulence model was used in these analyses which has shown successful results simulating these cases numerically. [Menzies, 2002] A complex flow regime was found to be formed. This regime was associated with shock waves forming at the cowl lip followed by shock reflections, a separation of the boundary layer beginning at the s-shape of the inlet, and an increment of the separation area towards the engine face. The results of this case showed a slight overprediction of the flow inside the inlet up to X/D=1.0, where the complex flow regime was formed.

In conclusion, it has been remarked that the results obtained from steady flow analyses are quite compatible with the previous experimental and numerical studies. Thus, it has been determined that the methods used are correct. The next step will be to perform flow analyses dependent on time. Then, it is planned to examine the Hammershocks that will occur in the channel associated with these analyses.

**Acknowledgments**

The authors would like to express their thanks to TUSAS (The Turkish Aerospace Industries) for their financial and technical support under project number 20201026-02 through their LIFT UP program, and TUBITAK (The Scientific and Technological Research Council of Turkey) for their financial support through the projects of TUBITAK 2209-B.

**References**

B.H. Anderson, D.R. Reddy, and K. Kapoor (1993) *A Comparative Study of Full Navier-Stokes and Reduced Navier-Stokes Analyses for Separating Flows Within a Diffusing Inlet S-Duct,* 29th AIAA, Monterey, California.

J. Becker, H. Bergmann, W. Luber (1994) *Dynamic Hammershock Effect on the Air Intake Design of Supersonic Aircraft*, Transactions on the Built Environment vol 8, 1994 WIT Press, ISSN 1743-3509.

William A. Benser and Harold B. Finger (1956) *Compressor Stall Problems In Gas-Turbine-Type Aircraft Engines*, SAE International, Vol. 65, 1957.

T. Breuer and S. Servaty (1996) ‘’*Stall inception and surge in high-speed axial flow compressors. In Loss Mechanisms and Unsteady Flows in Turbomachines*,’’ pages 26/1-26/17. AGARD CP-571.

C. R. Dawson (1971) “*Simulation and Measurement of Pressure Transients in a Mixed-Compression Supersonic Intake During Engine Surge*,” *Most*, no. 71.

M. J. Hinton, C. N. Eastlake (1998) *The Construction and Flight Testing of a Scaled, Remotely-Piloted, Flight-Test Vehicle*, Cessna Aircraft Company, Embry-Riddle Aeronautical University, Session 2206.

A. P. Kurkov, R. H. Soeder, and J. E. Moss, “*Memorandum Nasa Tm X-71594 I Nvesti Gat 1 on of the Stall- I Nduced Shock Wave ( Hammer Shock ) At the I Nlet To the Engine*,” vol. 71594.

G. Laurelle (2002) *Air Intakes: Role, Constraints and Design*, EADS Launch Vehicles, ICAS 2002 Congress, Publisher, International Council of the Aeronautical Sciences, Les Mureaux, France.

F. L. Marshall (1973) “*Prediction of Inlet Duct Overpressures Resulting from Engine Surge*.”

R. D. D. Menzies (2002) *Investigation Using S-Shaped of Computational Intake Fluid Aerodynamics Dynamics,* University of Glasgow, for the Degree of Doctor of Philosophy University of Glasgow.

D. N. Miller, J. W. Hamstra, and F. Worth (1996) “*A Computatıonal Assessment of Surge-Induced Inlet Overpressure Presented at the International Gas Turbine and Aeroengine Congress & Exhibition’’* Birmingham , UK — June 10-13 , 1996, pp. 1–9.

J. Nugent, J. K. Holzman (1974) *Flight- Measured Inlet Pressure Transients Accompanying Engine Compressor Surges on the F-111A Airplane*, NASA TN D-7696, National Aeronautics and Space Administration, Washington, D.C.

D. Ramasamy, S. Mahendran, Zamri.M, S.Vijayan (2009) *Design Optimization of Air Intake System (AIS)*, Faculty of Mechanical Engineering, Universiti Malaysia Pahang, 26300, Pekan, Pahang, Malaysia.

A. Robert (2002) “*On Hammershock in a Supersonic Propagation Flow*,” no. July.

H. K. Versteeg, W. Malalasekera (1995) *An Introduction to Computational Fluid Dynamics*, Bell and Brain Limited, Glasgow.

D. C. Wilcox (2013) “*Turbulence Modelling for CFD*,” *J. Chem. Inf. Model.*, vol. 53, no. 9, pp. 1689–1699.

L. C. Young and W. D. Beaulieu (1975) “*Review of hammershock pressures in aircraft inlets*,” *J. Aircr.*, vol. 12, no. 4, pp. 210–216, doi: 10.2514/3.44435.

Q. Zhang, P. Yan, J. Li, J. Lei, and A. G. Equations (2017) “10008269,” vol. 11, no. 12, pp. 1829–1838.